Draft version March 25, 2021
Typeset using LaTeX default style in AASTeX62

Hot and Cold Cases for SOC-i Thermal Analysis (v1)

Boone Tate, Željko Ivezić[1]

[1] *University of Washington, 3910 15th Avenue NE, Seattle, WA 98195, USA*

ABSTRACT

We computed temperature variation with time for the SOC-i satellite using a variety of input assumptions. The computation is based on a simple model for the satellite temperature variation with time when the satellite is subjected to a bistable heat source: two orbital segments with piece-wise constant power. The model assumes that at a given time a single temperature applies to the entire satellite body. We defined the so-called "hot" and "cold" cases and found that the low and high temperature extremes for a randomly oriented SOC-i satellite are −14 °C and +17 °C. When the satellite orientation is deliberately chosen to maximize the temperature extremes, the corresponding values are −38 °C and +42 °C. These results, and the allowed operating temperature ranges for satellite components imply that low temperatures will be more worrisome than high temperatures. We also explored a toy model for active temperature control that assumes an additional internal power dissipation whenever the satellite temperature drops below a pre-defined threshold, and concluded that such an approach is a viable method for mitigating low temperatures. These results are sensitive to assumed specific heat, which we simply assumed to correspond to aluminum, and should be revisited with more accurate input values.

Keywords: Satellites — CubeSat — SOC-i — Radiative transfer — Thermal model

1. INTRODUCTION

When designing a satellite such as SOC-i, it is crucial to establish that the temperature variation for each component will be within its operating range. In practice, professional engineering tools and numerical analysis are used to analyze complex systems. The SOC-i team utilizes the code Ansys to predict satellites temperature distribution. In order to compute temperatures, Ansys requires as input numerical specifications for the sources of radiation that SOC-i absorbs. In addition, the satellite's orbital parameters and orientation are also required. Given that the details of SOC-i orbit will not be known until its launch, here we define the so-called "hot" and "cold" cases which capture scenarios that predict the coldest and the hottest satellite temperatures.

In addition, we computed SOC-i temperature variation with time for hot and cold cases using a simple model that assumes that a single temperature applies to the entire satellite body at any given time. Although simple, this modeling produces approximately correct temperature estimates and deep physical insight, and can be used for fast studies of the impact of various input assumptions on the resulting satellite temperature. Most importantly, these results provide a "sanity check" for the more sophisticated, but also more prone to input errors, Ansys models.

The main quantitative result of the models presented here is that it is much more likely for low than for high temperatures to present problems for SOC-i operations phase. Motivated by this finding, we also explored a toy model for active temperature control that assumes an additional internal power dissipation whenever the satellite temperature drops below a pre-defined threshold.

In the next section, we first describe our mathematical model and input parameters, and then discuss specific results obtained with input parameters corresponding to SOC-i. In §3, we present a toy model for active temperature control, and summarize our findings in §4.

2. THERMAL ANALYSIS FOR SOC-I

The mathematical model for thermal analysis is discussed in detail in an accompanying document (Ž. Ivezić, 2021, unpublished, hereafter I21). Here we extend analysis from a bistable heat source discussed there to an arbitrary heating pattern along the orbit, including a temperature-driven additional internal power dissipation. For this reason,

Table 1. Surface optical absorptivity and infrared emissivity for SOC-i surface materials.

Part	Surface	α	ϵ	k ($\mathrm{W\,m^{-1}\,K^{-1}}$)	C ($\mathrm{J\,kg^{-1}\,K^{-1}}$)
Solar panels	GaAs, with AR coating	0.92	0.85	60.6	324
Al panels, outside	7075 Al, Kapton	0.87	0.81	121.2	801
Al frame rails	5052 Al, hard anodized	0.86	0.86	138.5	768
Al frame	5052 Al, alodine	0.08	0.15	138.5	768
PCBs	FR4	0.81	0.90	18.0	1544

we had to resort to a numerical solution of the governing differential equation (see eq. 1 in I21, hereafter I21-eq1). A sufficient accuracy of numerical solution was verified using analytic solution for a case with piecewise constant bistable heat source (I21-eq17).

Model input parameters include environmental, orbital and satellite parameters, all of them subject to appreciable uncertainties. At least in principle, orbital and satellite parameters are deterministic and should not have any uncertainties. However, detailed orbital information is sometimes unknown until the launch, and satellite orientation might be subject to operational uncertainties. We first describe SOC-i physical parameters used in computations here, and then discuss orbital and environmental parameters, including definitions of the so-called "hot" and "cold" cases that attempt to account for various modeling uncertainties. After all the input parameters are introduced, we discuss the results of thermal modeling.

2.1. *Input satellite parameters*

We used the SOC-i CAD model developed for structural analysis to extract information about external satellite surfaces and their material properties. We adopted the following description of external SOC-i surfaces:

- Top: 60% solar panel, 40% aluminum frame
- Bottom: 38% aluminum frame, 62% PCB (printed circuit board).
- Sides (2): 64% solar panels, 19% aluminum panels (outside), 17% aluminum frame rails
- Sides (2): 57% solar panels, 26% aluminum panels (outside), 17% aluminum frame rails

With the values of absorptivity and emissivity listed in Table 1, we obtained their surface-weighted values $\alpha = 0.83$ and $\epsilon = 0.79$ (54% of external surface area is covered by solar panels). In addition, we assumed that the satellite mass is $m = 2.6$ kg and adopted specific heat corresponding to aluminum ($C = 768\ \mathrm{J\,kg^{-1}\,K^{-1}}$), yielding a thermal intertia of $mC = 2.00\ \mathrm{kJ\,K^{-1}}$. This value of thermal intertia needs to be varified with detailed modeling (e.g., summing the mC product for all individual structural components in the SOC-i CAD model).

2.2. *Assumptions for orbital parameters*

It is already known that SOC-i will have a nearly-polar sun-synchronous orbit[1] with an altitude of $h = 550$ km and orbital inclination of 97.7 degrees. A satellite in sun-synchronous orbit passes over any given point of the planet's surface at the same local mean solar time because the orbit precesses through one complete revolution each year (that is, the orbit always maintains the same relationship with the Sun).

The eclipse duration for sun-synchronous orbits depends on their right ascension of the ascending node (RAAN), which will not be known until the launch date (RAAN is determined by the exact launch time). The orbital period for sun-synchronous orbit with an altitude of $h = 550$ km is 96 mins, and the maximum eclipse duration is 36 mins. When the orbital plane is perpendicular to incoming solar radiation, there is no eclipse (the satellite is following the terminator line at all times).

2.3. *The concept of hot and cold cases*

Due to uncertainties in input parameters, including environmental, orbital and satellite parameters, engineering pre-launch analysis often focuses on most extreme scenarios that predict the coldest and the hottest satellite temperatures. We define "hot" and "cold" cases by first adopting the extreme values of environmental parameters from Table 2.

[1] See https://en.wikipedia.org/wiki/Sun-synchronous_orbit

Table 2. The range of input enviromental parameters.

Quantity	max	min	mean	unit
Solar flux	1422	1322	1372	Wm^{-2}
Earth albedo	35	25	30	%
Earth IR flux	260	220	240	Wm^{-2}

Table 3. Absorbed flux ($\alpha = 0.83$) for hot and cold cases (in Wm^{-2}).

Quantity	hot case	cold case	ratio hot/cold
Direct solar flux	1181	1098	1.08
Reflected solar flux	21.0	144.2	0.15
Earth IR flux	174.6	147.8	1.18

In addition, we make an assumption that the orientation of SOC-i's sun-synchronous orbit results in an eclipse with maximum duration (36 min) for cold case, and no eclipse at all for hot case.

The intensity of solar radiation reflected from Earth varies along the orbit (I21-eq6). For a polar orbit passing through subsolar point, $f_{alb} = 0.62$ for the non-eclipsed part of the orbit, while for a polar orbit aligned with the terminator (with no eclipse), $f_{alb} = 0.06$. Therefore, we adopt $f_{alb} = 0.62$ for hot case and $f_{alb} = 0.06$ for cold case (note that reflected solar radiation contributes more flux for cold case, when not in eclipse).

With these assumptions, we use equations 3–13 from I21 to compute incoming heating flux. For cold case, the only heating flux during the eclipsed portion of the orbit is IR flux from Earth. The variation of flux between hot and cold cases for three main heat sources is summarized in Table 3. Note that reflected solar flux is smaller for hot case but this difference is compensated by the absence of eclipsed orbital portion in hot case.

Table 3 lists absorbed flux per unit area, assuming SOC-i's effective absorption coefficient (α). **The listed value are also appropriate for detailed Ansys-based modeling, but need to be corrected for α of each surface material.** The actual absorbed power (absorbed energy per unit time) depends on the values of η_S and η_E, which in turn depend on orientation. We make additional assumptions about satellite orientation, as discussed next.

2.4. *Assumptions for satellite orientation*

The satellite orientation determines effective surface areas for the absorption of radiation from the Sun and Earth. For convenience, these surface areas are expressed relative to the total surface area, A_{tot} (=0.1 m^2 for SOC-i), using η factors (η_S and η_E, respectively). For a given orbit and satellite orientation, η_S and η_E can be computed by adding corresponding values (known as "view factors") for six individual sides (see Appendix A in I21).

We used results discussed in Section 2.4 from I21 to adopt the following values for SOC-i. When averaged over plausible orientations and orbits, $\eta_S = 0.21$ and $\eta_E = 0.36$, with an uncertainty due to actual orbit specifics of the order 10%. The limits of possible ranges are $\eta_S = 0.10 - 0.30$ and $\eta_E = 0.34 - 0.38$. The limits for η_S reflect the range of projected area towards plane-parallel rays for 2U CubeSat geometry, with the minimum value corresponding to one small side oriented perpendicularly to the incoming solar radiation. For η_E, the variation is much smaller because typically all six sides can "see" Earth's surface[2].

We do not adopt specific satellite orientation for hot and cold cases but instead explore two options in each case. First, we adopt averaged orientations for both hot and cold cases, with $\eta_S = 0.21$ and $\eta_E = 0.36$ corresponding to 2U CubeSat values. As the second assumption, we consider the following extreme cases: $\eta_S = 0.30$ and $\eta_E = 0.34$ for hot case, and $\eta_S = 0.10$ and $\eta_E = 0.38$ for cold case.

The second set of values assumes that the satellite orientation is actively controlled. For hot case, the maximum possible projected satellite area for plane-parallel rays is always pointing towards the Sun ($\eta_S = 0.30$). For cold case and during non-eclipsed portion, the smallest satellite side is always pointing towards the Sun ($\eta_S = 0.10$). The adopted values of η_E are its extreme values.

[2] We note that even for spherical geometry η_S and η_E are generally different: $\eta_S = 1/4$, while η_E decreases from 1/2 to 1/4 as the orbit altitude varies from zero to infinity.

Table 4. Absorbed power (in Watt) and equilibrium temperatures for hot and cold SOC-i cases.

Quantity	hot, random	hot, extreme	cold, random	cold, extreme
Absorbed direct solar	24.8	36.6	23.1	11.0
Absorbed Earth albedo	0.8	0.8	5.2	4.9
Absorbed Earth IR	6.3	6.6	5.3	5.0
Internal dissipation	5.1	7.5	3.5	2.0
Total input in eclipse	—	—	8.9	7.0
Total input in sun	31.8	44.0	31.4	19.7
Equilibrium T in eclipse	—	—	211	199
Equilibrium T in sun	290	315	289	257
T_{min} (K)	290	315	259	235
T_{max} (K)	290	315	274	244
T_{min} (°C)	16.7	41.5	**−14.2**	**−37.6**
T_{max} (°C)	**16.7**	**41.5**	1.3	−28.9

2.5. *Assumptions for internal power dissipation*

A fraction of absorbed optical flux (the sum of direct solar flux and reflected solar flux) is often used to charge on-board batteries. We assume that 20% of absorbed flux[3] is converted into chemical energy ($\eta_{cell} = 0.2$). This energy is returned back at a constant rate as internal heat dissipation.

In hot case, satellite is always exposed to the Sun and there is **no net effect** within the context of single-temperature model considered here. In reality, and in detailed Ansys models, this internal heat dissipation can modify the temperature distribution within the satellite (areas closer to the heater will have elevated temperature). In cold case, the effect of internal heat dissipation is to **minimize** the amplitude of temperature variation, or equivalently, to raise the minimum temperature (at the end of eclipsed portion).

These assumptions complete the specification of hot and cold thermal models. We proceed with a discussion of numerical results.

2.6. *Predicted absorbed power and equilibrium temperatures for hot and cold cases*

Given all the input assumptions described in the previous section, it is straightforward to solve the governing equation with direct numerical integration (I21-eq1). Table 4 lists predicted absorbed power for all four modeled cases. We note that the total energy stored in batteries, and dissipated as heat at a constant rate, ranges from 3.2 Wh for cold, extreme case to 12 Wh for hot, extreme case.

Predicted equilibrium temperatures (I21-eq14) range from 199 K to 317 K. In hot case, because there is no eclipse, these equilibrium temperatures also correspond to steady-state satellite temperature. However, in cold case, the high and low equilibrium temperatures only determine the average orbital temperature (I21-eq19). The actual amplitude of temperature variation is determined by the satellite heat capacity, or thermal inertia; as thermal inertia increases, the amplitude of temperature variation decreases.

2.7. *Predicted SOC-i temperature variation for hot and cold cases*

The left panel in figure 1 shows the SOC-i orbital temperature variation for "hot" and "cold" cases. The low and high temperature extremes for a randomly oriented SOC-i satellite are −14 °C and +17 °C (see T_{min} and T_{max} in Table 4). The right panel shows the temperature variation when the satellite orientation is deliberately chosen to maximize the temperature extremes; the corresponding values are −38 °C and +42 °C.

3. ACTIVE TEMPERATURE CONTROL

Given the allowed operating temperature ranges for satellite components (the most stringent requirement comes from batteries, chosen here as 0–40 °C for illustration), these results imply that low temperatures will be more worrisome than high temperatures. Motivated by this finding, we explored a model for active temperature control.

[3] Here, η_{cell} represents the fraction of all absorbed radiation that was converted to battery charge. For example, if the cells occupy 2/3 of all external surfaces, and the cell conversion efficiency is 30%, then η_{cell}= 0.2. For randomized orientiations, it's only "effective" quantities that count in the model considered here; however, when a specific satellite orientation is known, one could incorporate information about where exactly the solar cell panels are positioned, too.

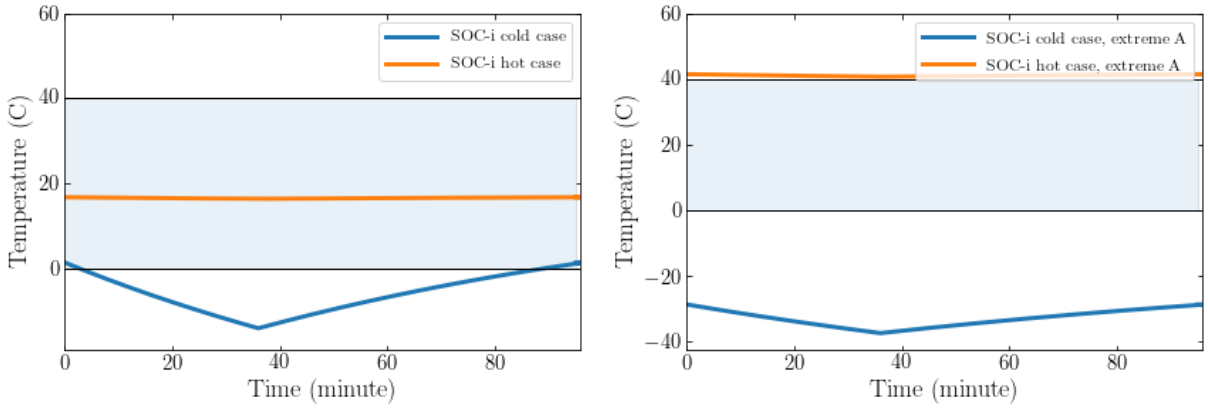

Figure 1. The impact of choosing extreme values of environmental conditions on SOC-i temperature, when assuming randomized satellite orientation (left), and with orientation that maximizes the temperature range between these so-called "hot" and "cold" cases (right). The temperature variation is compared to a typical battery operating temperature range (the blue horizontal band). For hot case, there is no temperature variation with time because the assumed orbit has no eclipsed portion.

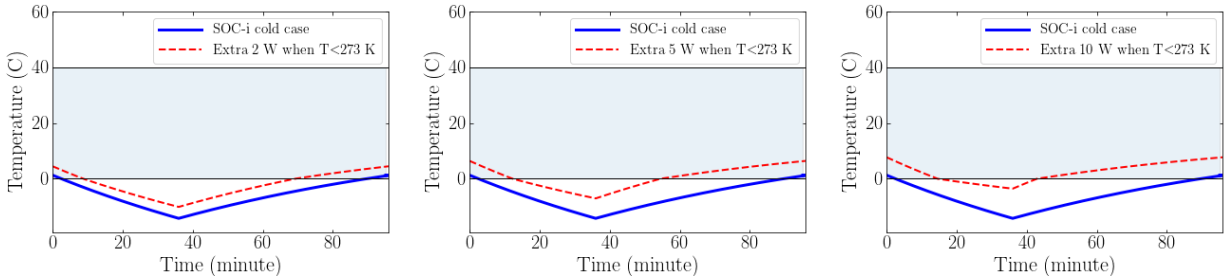

Figure 2. Illustration of the impact of active thermal control. A toy model assumes that whenever the satellite temperature drops below zero °C (273 K), an additional heating source with power of 2 W (left), 5 W (middle), or 10 W (right) contributes to the heat balance. The blue lines correspond to the blue line in the left panel in figure 1 (cold case) and the red dashed line is the corresponding temperature prediction with this additional heating power. The consumed power is about 1.9 Wh, 3.4 Wh and 4.3 Wh, respectively (the total available battery power is 5.6 Wh).

3.1. *A toy model for active temperature control*

We developed a toy model for active temperature control that assumes an additional internal power dissipation whenever the satellite temperature drops below a pre-defined threshold. We investigated cold case and three levels of power (2 W, 5, W, 10 W) that is applied whenever the temperature drops below 273 K (0 °C). Results are shown in figure 2.

Additional power can raise the satellite temperature by 5 to 11 degrees. The consumed power ranges from 1.9 Wh to 4.3 Wh, and it is under the total available battery power (5.6 Wh for cold case and $\eta_{cell} = 0.2$; for hot, extreme case, it could be boosted to 18 Wh with $\eta_{cell} = 0.3$). These results show that such an approach is a viable method for mitigating low temperatures.

4. CONCLUSIONS

We computed temperature variation with time for SOC-i satellite using a model with a single temperature that applies to the entire satellite surface at any given time, and a variety of input assumptions.

We defined the so-called "hot" and "cold" cases and found that the low and high temperature extremes for a randomly oriented SOC-i satellite are −14 °C and +17 °C. When the satellite orientation is deliberately chosen to maximize the temperature extremes, the corresponding values are −38 °C and +42 °C.

Within the model limitations, these estimates are accurate to within a few degrees. The results are sensitive to assumed specific heat, which we simply assumed to correspond to aluminum.

Since it appeared that low temperatures will be more concerning than high temperatures, we also explored a toy model for active temperature control that assumes an additional internal power dissipation whenever the satellite

temperature drops below a pre-defined threshold. We found out that such an approach is a viable method for mitigating low temperatures.

Without more detailed and robust SOC-i orbit and orientation descriptions, this model cannot be appreciably improved. Nevertheless, significant additional insight can be gained from Ansys models that are capable of computing temperature field throughout the satellite body. For external heat fluxes, values listed in Table 3 can be used but **they need to be corrected for different values of absorption coefficient (α) for each surface material.**

It would be prudent to first start with hot case because there is no temperature variation along the orbit and thus much faster steady-state Ansys calculation can be utilized. Once that case is verified to be in approximate agreement with the results presented here (in particular, we expect that the mean external surface temperature of 17 °C for random orientations should be reproduced to within a few degrees), transient thermal analysis should be attempted for cold case.

The latex source for this document, and the supporting python code, are publicly available[4].

References

Gilmore, D. 2002, "Spacecraft Thermal Control Handbook: Fundamental Technologies", 2nd ed. Aerospace Press

Hengeveld, D.W. et al. 2009, "Hot- and Cold-Case Orbits for Robust Thermal Control", Journal of Spacecraft and Rockets, Vol. 46, No. 6

Jacques, L. 2009, "Thermal Design of the Oufti-1 Nanosatellite", Master Thesis, University of Liege

Kang, S-J. & Oh, H-U. 2016, "On-Orbit Thermal Design and Validation of 1 U Standardized CubeSat of STEP Cube Lab", International Journal of Aerospace Engineering, Vol. 2016, Article 4213189

Kellens, A. 2018, "Thermal design of the OUFTI-Next mission", Master thesis, University of Liege

[4] https://github.com/ivezic/CubeSats